Electric Excitation of Spin Resonance in Antiferromagnetic Conductors

Revaz Ramazashvili
Department of Physics and Astronomy, University of South Carolina, Columbia, SC 29208, USA
(Dated: August 8, 2009)

Antiferromagnetism couples electron spin to its orbital motion, thus allowing excitation of electron spin transitions by an AC *electric* rather than magnetic field – with absorption, exceeding that of common electron spin resonance (ESR) at least by four orders of magnitude. In addition to potential applications in spin electronics, this phenomenon may be used as a spectroscopy to study antiferromagnetic materials of interest – from chromium to borocarbides, cuprates, iron pnictides, organic and heavy fermion conductors.

PACS numbers: 75.50.Ee,76.30.-v,76.40.+b,71.70.Ej

I. INTRODUCTION

Broad research effort has been underway [1, 2, 3] to build a new generation of electronic devices, that would manipulate and monitor carrier spin and charge on an equal footing. Magnetic semiconductors [4, 5] and giant magnetoresistance materials [6], as well as semiconductors with spin-orbit interaction [7], have been much scrutinized with this goal in mind.

By contrast, antiferromagnets have enjoyed far less attention in this context. Here, I show that, in fact, antiferromagnets in their ordered state may prove useful for spin manipulation by electric field, as antiferromagnetism couples electron spin to its orbital motion. This coupling manifests itself especially vividly in a magnetic field, where it takes the form of anisotropic Zeeman interaction with a momentum-dependent g-tensor. This dependence turns a common Zeeman term into a spin-orbit coupling $\mathcal{H}_{ZSO}$:

$$\mathcal{H}_{ZSO} = -\mu_B \left[g_\parallel (\mathbf{H}_\parallel \cdot \boldsymbol{\sigma}) + g_\perp(\mathbf{p}) (\mathbf{H}_\perp \cdot \boldsymbol{\sigma}) \right] . \qquad (1)$$

Hereafter, $\mathbf{H}_\parallel = (\mathbf{H} \cdot \mathbf{n})\mathbf{n}$ and $\mathbf{H}_\perp = \mathbf{H} - \mathbf{H}_\parallel$ are the longitudinal and transverse components of the magnetic field $\mathbf{H}$ with respect to the unit vector $\mathbf{n}$ of the staggered magnetisation, μ_B is the Bohr magneton, while $g_\parallel$ and $g_\perp(\mathbf{p})$ are the longitudinal and transverse components of the g-tensor. While $g_\parallel$ is momentum-independent up to small relativistic corrections, $g_\perp(\mathbf{p})$ has a set of zeros in the Brillouin zone and thus substantially depends on the quasiparticle momentum momentum $\mathbf{p}$. This remarkable fact is dictated by the symmetry of antiferromagnetic state [8, 9, 10], and gives rise to a number of interesting effects.

One such effect amounts to excitation of spin resonance transitions by an AC *electric* field, with resonance absorption exceeding that of common electron spin resonance (ESR) by over four orders of magnitude. This phenomenon does not rely on the presence of localized magnetic moments, and is possible both for itinerant electrons and for impurity-bound electron states. Hence it can be used as a resonance spectroscopy, tailor-made to study antiferromagnets of great interest from chromium to cuprates, borocarbides, iron pnictides, as well as organic and heavy-fermion materials.

II. THE SPECTRUM

Here, I illustrate this effect by an example, that may be relevant to a number of antiferromagnetic conductors: I study electric excitation of *itinerant*-electron resonance in a weakly-doped two-dimensional antiferromagnetic insulator on a lattice of square symmetry, whose conduction band minimum falls at the center Σ of the magnetic Brillouin zone (MBZ) boundary, as shown in Fig. 1(a). Both the two-dimensionality and the square symmetry of this example simplify the description and make it relevant to materials such as cuprates and iron pnictides, yet neither of the two features is essential to the effect. Numerous other antiferromagnets of different crystal symmetry and effective dimensionality are discussed in Ref. [10]. Magnetic field is assumed small on the scale of the electron excitation gap Δ and of the reorientation threshold, and thus does not perturb antiferromagnetic order.

The effect is most vivid for the staggered magnetization axis $\mathbf{n}$, pointing along the conducting plane, which is the case in several electron-doped cuprates [11, 12]. The magnetic field $\mathbf{H}$ is nearly normal to $\mathbf{n}$, which tends to happen due to spin-flop. It is this very geometry that I consider hereafter; orientation of the field with respect to the conducting plane may be arbitrary, as shown in Fig. 1(b).

At low doping, the carriers concentrate in a small vicinity of the band minimum Σ, and the Hamiltonian can be expanded around it. By symmetry, $g_\perp(\mathbf{p})$ in $\mathcal{H}_{ZSO}$ (1) vanishes upon approaching the MBZ boundary, linearly in a generic case [9, 10] – and can be recast as $g_\perp(\mathbf{p}) = g_\parallel \frac{p_y \xi}{\hbar}$ with a constant ξ, for $\frac{p_y \xi}{\hbar} \ll 1$. Here, p_y is the component of the momentum deviation from the band minimum, locally transverse to the MBZ boundary, as shown in Fig. 1(a). The length scale ξ is of the order of the antiferromagnetic coherence length $\hbar v_F/\Delta$, and may be of the order of the lattice constant or much greater [9, 10].

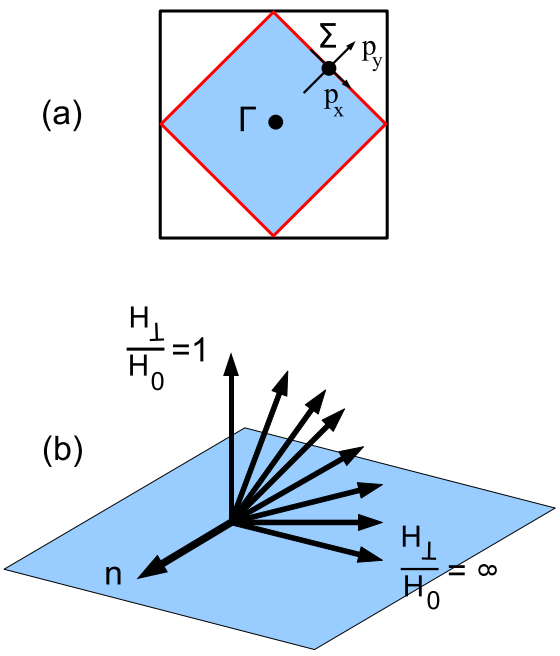

FIG. 1: (color online). Geometry of the problem. (a) The Brillouin zone of a Néel antiferromagnet on a lattice of square symmetry, and its magnetic Brillouin zone (MBZ, shaded diagonal square). The line of zero $g_\perp(\mathbf{p})$ must contain the entire MBZ boundary, shown in red online. Point Γ is the Brillouin zone center, point Σ is the center of the MBZ boundary, where the conduction band minimum is assumed to occur, and p_y is the component of the momentum deviation from the minimum, locally transverse to the MBZ boundary. (b) Real-space geometry: staggered magnetisation axis $\mathbf{n}$, pointing along the conduction plane, and nearly transverse magnetic field $\mathbf{H}$, here drawn normal to $\mathbf{n}$; components $H_\perp$ and H_0 are normal to $\mathbf{n}$ and to the conducting plane, respectively.

Near the band minumum, the kinetic energy is quadratic in $\mathbf{p}$; for simplicity, I consider isotropic effective mass m, and introduce $\mathbf{\Omega} \equiv \mu_B g_\parallel \mathbf{H}$. For the field at a finite angle with the conducting plane, the Hamiltonian reads

$$\mathcal{H} = \frac{1}{2m}\left[\mathbf{p} - \frac{e}{c}\mathbf{A}\right]^2 - (\mathbf{\Omega}_\parallel \cdot \boldsymbol{\sigma}) - \frac{\xi}{\hbar}\left[\mathbf{p} - \frac{e}{c}\mathbf{A}\right]_y (\mathbf{\Omega}_\perp \cdot \boldsymbol{\sigma}), \tag{2}$$

where $\mathbf{A}$ is the electromagnetic vector potential [13].

In a purely transverse field ($\mathbf{\Omega}_\parallel = 0$), the up- and the down-spin projections onto $\mathbf{\Omega}_\perp$ decouple and have identical Landau spectra:

$$\mathcal{E}_n = \Omega_0\left[n + \frac{1}{2}\right], \tag{3}$$

where $\Omega_0 \equiv \hbar\frac{eH_0}{mc}$ is the cyclotron energy, and H_0 is the normal component of the field with respect to the conducting plane. This degeneracy becomes explicit upon completing the square in Eqn. (2) with respect to $[\mathbf{p} - \frac{e}{c}\mathbf{A}]_y$, or upon performing a non-uniform spin rotation

$$\Psi \to \exp\left[i\frac{y}{\hbar}\frac{m\xi}{\hbar}(\mathbf{\Omega}_\perp \cdot \boldsymbol{\sigma})\right]\Psi, \tag{4}$$

which, in a purely transverse field ($\mathbf{\Omega}_\parallel = 0$), eliminates $\mathbf{\Omega}_\perp$ from the Hamiltonian altogether.

In the Landau gauge $\mathbf{A} = (0, xH_0)$, this spin degeneracy in a transverse field acquires a simple interpretation: as shown in Fig. 2, the guiding orbit centers of the spin-up and the spin-down states split apart by the distance $\lambda \equiv 2\xi\frac{\Omega_\perp}{\Omega_0}$ along the $\hat{x}$ axis in real space, with the spin quantization axis chosen along $\mathbf{\Omega}_\perp$.

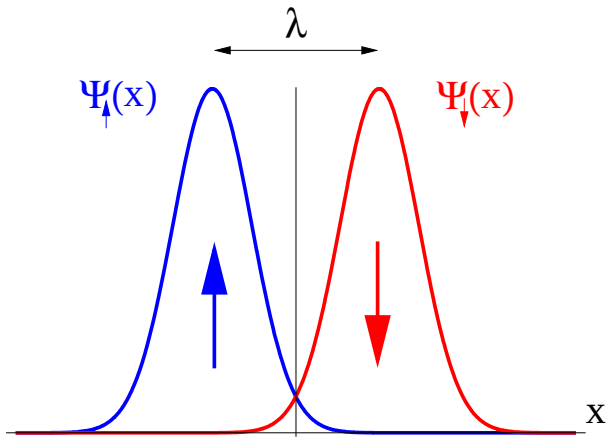

FIG. 2: (color online). Splitting of degenerate spin states in real space: the spin 'up' state $\Psi_\uparrow(x)$ and the spin 'down' state $\Psi_\downarrow(x)$ at the lowest Landau level, with the spin quantization axis chosen along $\mathbf{\Omega}_\perp$. In a purely transverse field ($\mathbf{\Omega}_\parallel = 0$), the two wave functions remain degenerate, but split by the distance $\lambda = 2\xi\frac{\Omega_\perp}{\Omega_0}$ along the $\hat{x}$ axis in real space.

To study the spectrum in an arbitrary field, it is convenient to use a different Landau gauge: $\mathbf{A} = (-yH_0, 0)$. The spin rotation (4) removes the transverse field term, and turns the uniform longitudinal field $\mathbf{\Omega}_\parallel$ into a spiral texture $\mathbf{\Omega}'_\parallel$ with a constant pitch $q \equiv \frac{2m\xi\Omega_\perp}{\hbar^2}$ along the $\hat{y}$-axis in the conducting plane:

$$\mathbf{\Omega}'_\parallel = \mathbf{\Omega}_\parallel \cos[qy] + \mathbf{n}_\perp \times \mathbf{\Omega}_\parallel \sin[qy], \tag{5}$$

where $\mathbf{n}_\perp$ is the unit vector along $\mathbf{\Omega}_\perp$. It is helpful to recast the cyclotron motion in terms of ladder operators as per $\frac{a+a^+}{\sqrt{2}} \equiv \frac{y}{l_H} - \frac{p_x l_H}{\hbar}$ and $\frac{a-a^+}{i\sqrt{2}} \equiv \frac{p_y l_H}{\hbar}$, where $l_H = \sqrt{\frac{\hbar c}{eH_0}}$ is the magnetic length. Now, the Hamiltonian (2) reads

$$\mathcal{H} = \Omega_0\left[a^+a + \frac{1}{2}\right] - (\mathbf{\Omega}'_\parallel \cdot \boldsymbol{\sigma}), \tag{6}$$

with y in $\mathbf{\Omega}'_\parallel$ of Eqn. (5) expressed via the ladder operators.

According to Eqn. (6), in the limit of a weak longitudinal field ($\Omega_\parallel \ll \Omega_0$), the spin precesses at a characteristic frequency $\Omega_\parallel$, which is small compared with the cyclotron frequency Ω_0 of the orbital motion. In this limit, the splitting $\delta\mathcal{E}_n$ of the n-th Landau level is given simply by averaging $(\mathbf{\Omega}'_\parallel \cdot \boldsymbol{\sigma})$ over the orbital eigenstate $|n\rangle$ of the first term in Eqn. (6), leading to

$$\delta\mathcal{E}_n = 2\Omega_\parallel f_n\left(\frac{\xi}{l_H}\frac{\Omega_\perp}{\Omega_0}\right), \qquad (7)$$

where $f_n(\zeta) = L_n(2\zeta^2)\exp[-\zeta^2]$, and $L_n(\zeta)$ is the Laguerre polynomial [14]. The degeneracy is lifted in a peculiar way: for $\Omega_\parallel \ll \Omega_0$, the splitting $\delta\mathcal{E}_n$ of the n-th Landau level decays and oscillates as a function of $\zeta = \frac{\xi}{l_H}\frac{\Omega_\perp}{\Omega_0}$, as shown in Fig. 3. For a small fixed $\Omega_\parallel \ll \Omega_\perp$, this amounts to decaying oscillations with reducing the angle between the field and the conducting plane, as shown in Fig. 1(b).

The factor $f_n(\zeta)$ in Eqn. (7) is of a simple origin. The longitudinal component $\mathbf{\Omega}_\parallel$ hybridizes the two states in Fig. 2 and lifts their degeneracy. Indeed, the splitting vanishes as the distance $\lambda = 2\xi\frac{\Omega_\perp}{\Omega_0}$ between the guiding orbit centers exceeds the wave function size $l_H\sqrt{n+1}$. The oscillations on the background of this decay are due to spatial oscillation of the two wavefunctions for $n > 0$.

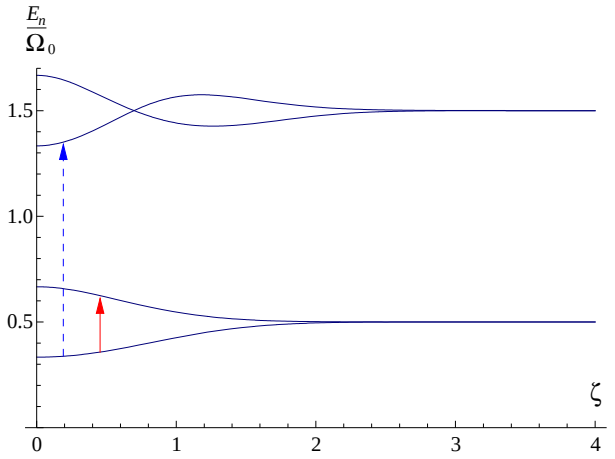

FIG. 3: (Color online) The Landau level splitting. The first two Landau levels E_n, split by the longitudinal field $\Omega_\parallel = \Omega_0/6$, are shown in units of Ω_0 as a function of $\zeta = \frac{\xi}{l_H}\frac{\Omega_\perp}{\Omega_0}$. The levels were obtained by numerical solution of the Hamiltonian (6), truncated to the lowest six levels. The solid arrow indicates the ZEDR transition at the lowest Landau level, whereas the dashed arrow corresponds to the cyclotron resonance transition from the lowest to the first Landau level.

III. ELECTRIC EXCITATION OF SPIN RESONANCE

The momentum dependence of $g_\perp(\mathbf{p})$ has a spectacular spectroscopic manifestation: excitation of spin resonance transitions by an AC *electric* field – the very same transitions that are normally excited by an AC magnetic field in an ESR experiment.

I name this phenomenon Zeeman Electric-Dipole Resonance (ZEDR) to note its similarity with Electric-Dipole Spin Resonance (EDSR) in semiconductors and semiconducting heterostructures with spin-orbit coupling [15].

A. Resonance in a quantizing field

To study the effect for discrete Landau levels, notice that a uniform AC electric field E^y_ω along the $\hat{y}$-axis couples to the y-component $ey = el_H\frac{a+a^+}{\sqrt{2}}$ of the electron dipole moment. With E^y_ω, the Hamiltonian (6) reads

$$\mathcal{H} = \Omega_0\left[a^+a + \frac{1}{2}\right] - (\mathbf{\Omega}'_\parallel \cdot \boldsymbol{\sigma}) - e\frac{a+a^+}{\sqrt{2}}l_H E^y_\omega. \qquad (8)$$

In the absence of a longitudinal component $\mathbf{\Omega}_\parallel$, the last term in (8) induces only the cyclotron resonance: spin-conserving electric dipole transitions between the adjacent Landau levels, with the matrix element M_{CR}

$$M_{CR} = \langle n+1,\sigma|eyE^y_\omega|n,\sigma\rangle = el_H E^y_\omega\sqrt{\frac{n+1}{2}}, \qquad (9)$$

whose scale is set by the Larmore radius $l_H\sqrt{n+1}$.

A small longitudinal component $\Omega_\parallel \ll \Omega_0$ changes this picture, as $(\mathbf{\Omega}'_\parallel \cdot \boldsymbol{\sigma})$ couples the electron spin to its orbital motion. As a result, the n-th Landau level eigenstate $|n\alpha\rangle$ with spin projection α on the direction of $\mathbf{\Omega}_\parallel$ acquires a small admixture of other states $|m\beta\rangle$, and the AC electric field begins to induce a number of previously forbidden transitions.

Here, I restrict myself to spin-flip transitions within the same Landau level [16], excited by an AC *electric* field as shown in Fig. (3). Treating the admixture of other Landau levels to the first order in $(\mathbf{\Omega}'_\parallel \cdot \boldsymbol{\sigma})$, one finds [17] the ZEDR matrix element $M_{ZEDR} \equiv \langle n\uparrow|eyE^y_\omega|n\downarrow\rangle$:

$$M_{ZEDR} = -2e\xi E^y_\omega\frac{\Omega_\parallel}{\Omega_0}\frac{\Omega_\perp}{\Omega_0}L_n(2\zeta^2)\exp\left[-\zeta^2\right], \qquad (10)$$

where $\zeta \equiv \frac{\xi}{l_H}\frac{\Omega_\perp}{\Omega_0}$. Apart from the dependence on the orientation of the field with respect to the conducting plane and to the staggered magnetization, ZEDR matrix elements are defined simply by the length scale ξ. Being at least of the order of the lattice spacing, in a weakly-coupled spin density wave antiferromagnet $\xi \sim \hbar v_F/\Delta$ (see Refs. [9, 10]) may reach a 10 nm scale [18]. At the same time, the ESR matrix elements are defined by the

Compton length $\lambda_C = \frac{\hbar}{mc} \approx 0.4$ pm. The characteristic ratio of the ZEDR matrix elements to those of ESR can thus be estimated as $\frac{\xi}{\lambda_C} = \frac{1}{\alpha}\frac{\xi}{a_B}$, where $a_B = \frac{\hbar^2}{me^2} \approx 53$ pm is the Bohr radius, and $\frac{1}{\alpha} = \frac{\hbar c}{e^2} \approx 137$ is the inverse fine structure constant. Thus, the ZEDR absorption exceeds that of ESR by about $\left[137 \cdot \frac{\xi}{a_B}\right]^2$, which amounts to at least four orders of magnitude.

B. Resonance in a continuous spectrum

Now, consider a situation, where the DC magnetic field **H** couples only to the electron spin, but not to its orbital motion, which is the case for a field along the conducting plane. According to Eqn. (2), the field splits the conduction band into two subbands $\mathcal{E}_\pm(\mathbf{p})$

$$\mathcal{E}_\pm(\mathbf{p}) = \frac{\mathbf{p}^2}{2m} \pm \sqrt{\Omega_\parallel^2 + \left[\frac{p_y\xi}{\hbar}\right]^2 \Omega_\perp^2}, \qquad (11)$$

and the AC field induces transitions between them.

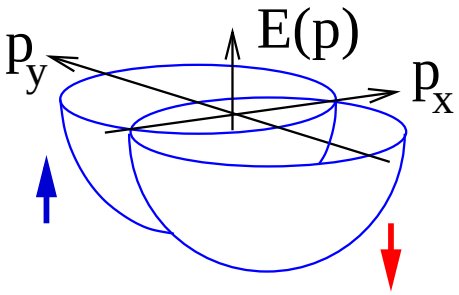

FIG. 4: (Color online) The spin splitting of the conduction band, sketched after Eqn. (12) in a small vicinity of the band minimum at point Σ.

According to (2), a purely transverse field ($\Omega_\parallel = 0$) lifts the Kramers degeneracy by splitting the two degenerate subbands by the 'distance' $\delta p_y = \frac{2}{\hbar} m\xi\Omega_\perp$ along the p_y-axis:

$$\mathcal{H} = \frac{p_x^2}{2m} + \frac{1}{2m}\left[p_y - \frac{m\xi}{\hbar}(\mathbf{\Omega}_\perp \cdot \boldsymbol{\sigma})\right]^2. \qquad (12)$$

Illustrated in Fig. 4, this is, indeed, a momentum-space counterpart of the real-space splitting in Fig. 2.

In the continuous spectrum, ZEDR may be treated simply as being induced by the term $\delta\mathcal{H}^\omega_{ZEDR} = \frac{\xi}{\hbar}\frac{e}{c}A^y_\omega(\mathbf{\Omega}_\perp \cdot \sigma)$. Its matrix element between the states with the spin along and against the direction of the effective magnetic field $(\mathbf{\Omega}_\parallel + \frac{\xi p_y}{\hbar}\mathbf{\Omega}_\perp)$ is equal to

$$|\langle\uparrow|\delta\mathcal{H}^\omega_{ZEDR}|\downarrow\rangle|^2 = \left[\frac{e\xi E^y_\omega}{\hbar\omega}\right]^2 \frac{\Omega_\parallel^2\Omega_\perp^2}{\Omega_\parallel^2 + \left[\frac{\xi p_y}{\hbar}\Omega_\perp\right]^2}, \qquad (13)$$

where I used the relation $\langle\downarrow|(\hat{n}\cdot\sigma)|\uparrow\rangle = n_+ \equiv n_x + in_y$ for an arbitrary unit vector $\hat{n}$.

The ZEDR absorption P^ω_{ZEDR} is given, according to the Fermi golden rule, by the product of the modulo squared (13) of the matrix element of $\delta\mathcal{H}^\omega_{ZEDR}$ by the AC field frequency ω, and by $\frac{\pi}{\hbar}$, with the subsequent summation over the Fermi surface, yielding

$$P^\omega_{ZEDR} = \frac{m}{\pi}\frac{[e\xi E^y_\omega]^2}{16}\frac{\sin^2\theta\cos^2\theta\left(\frac{\omega_H}{\hbar\omega}\right)^4}{\sqrt{\left(\left[\frac{\omega_H}{\hbar\omega}\right]^2\left[\cos^2\theta + 2\mu m\xi^2\sin^2\theta\right] - 1\right)\left(1 - \left[\frac{\omega_H}{\hbar\omega}\right]^2\cos^2\theta\right)}}, \qquad (14)$$

where μ is the electron chemical potential counted from the bottom of the band, and $\omega_H \equiv 2\Omega$. The result [19] is presented in a form, corresponding to sweeping the magnitude of the DC field at a fixed angle θ to the staggered magnetisation **n** and at a fixed frequency ω. In agreement with Eqn. (10), the ZEDR matrix elements are again defined simply by the lengthscale ξ.

The lineshape described by Eqn. (14) is intrinsically broadened: according to Eqn.(11), in a magnetic field of a generic orientation, each point at the Fermi surface has its own resonance frequency. Hence the absorption is non-zero in a finite interval of frequencies, with square-root singularities at the edges. This intrinsic broadening may be a reason behind the ESR silence of the cuprates [20].

IV. DISCUSSION AND CONCLUSIONS

Electric excitation of spin resonance becomes possible due to a substantial variation of the g-tensor across the Brillouin zone. In antiferromagnetic conductors, this variation is imposed by symmetry [8, 9, 10]. Hence, ZEDR shall be found in a broad range of materials from weakly-doped antiferromagnetic insulators to antiferromagnetic metals. Quantitative details between these two limits may vary, but the key sufficient condition for ZEDR amounts to a significant variation of $g_\perp(\mathbf{p})$ for the actual carriers.

Zeeman Electric-Dipole Resonance is induced by an AC electric field; to study it, a small sample has to be placed in a resonator at the electric field maximum. This puts ZEDR in competition against cyclotron resonance (CR), the latter generally being a stronger effect. Nevertheless, these two resonances can be easily distinguished.

Firstly, the CR and the ZEDR frequencies are different. In a nearly transverse field ($\Omega_\parallel \ll \Omega_0$), the former is simply the cyclotron frequency Ω_0 up to small corrections of the order of $\Omega_\parallel/\Omega_0 \ll 1$, as shown in Fig. 3. The ZEDR frequency is much smaller, of the order of $\Omega_\parallel \ll \Omega_0$, and shows the peculiar dependence (7) on the magnetic field strength and orientation.

Secondly, the ZEDR absorption grows with increasing the magnetic field and, already in a low field $\Omega_0 \sim \frac{\Delta^2}{\epsilon_F}$, becomes of the same order of magnitude as that of cyclotron resonance: this follows from Eqns. (9) and (10) [21]. For materials with $\Delta \ll \epsilon_F$, this crossover scale is small compared with Δ, which means that the ZEDR intensity may exceed that of the cyclotron resonance while the field is still much smaller than Δ, and hence does not perturb the antiferromagnetic order. This makes an antiferromagnetic conductor with a small ratio $\frac{\Delta}{\epsilon_F} \ll 1$ a promising candidate for the observation of ZEDR.

This condition is met by a number of materials from weakly-doped antiferromagnetic insulators to antiferromagnetic metals with a large Fermi surface. Among the latter, the simplest of opportunities to observe ZEDR may be offered by chromium [22], an archetypal spin density wave metal, ever attracting much attention [23].

Among systems more complex, oxychlorides [24] and electron-doped cuprates [25] have recently shown the appearance of carriers near the point Σ at the MBZ boundary at low doping, which may allow ZEDR, provided that the antiferromagnetic correlations are developed well enough. A number of other relevant materials are discussed in [10].

A. Experimental issues

In this subsection, I discuss a number of issues, that may be important for a successful observation of electrically-excited electron spin resonance in an antiferromagnetic conductor.

Since the effect hinges on a substantial momentum dependence of the g-tensor, it requires clean samples. Observation of de Haas–van Alphen oscillations could serve as an experimental criterion of a sufficient sample purity. Similarly, it is desirable to work with single-magnetic-domain samples.

Thermal fluctuations of the antiferromagnetic order reduce the ordered magnetization and scatter the charge carriers; at the same time, directional fluctuations of the staggered magnetization make the resonance frequency scale $\Omega_\parallel$ vary in space, leading to an additional smearing of the resonance. These effects can be suppressed by working well below the Néel temperature.

The theory above implicitly assumed, that the orientation of the field $\mathbf{H}$ with respect to the staggered magnetization $\mathbf{n}$ and to the conducting plane may be varied at will. This requires a sufficient magnetic anisotropy to maintain the orientation of $\mathbf{n}$ with respect to the crystal axes, or otherwise spin-flop would re-orient $\mathbf{n}$ transversely to $\mathbf{H}$. Therefore, $\mathbf{H}$ must be kept below the reorientation field of the material.

At the same time, the magnetic anisotropy helps to separate the electron spin resonance frequency from that of the antiferromagnetic resonance [26]: the former scales with $\Omega_\parallel$, while the latter scales as the square root of the anisotropy and thus remains finite at zero field. Possible interference with antiferromagnetic resonance is conveniently suppressed even further due to the fact that antiferromagnetic resonance is excited by an AC *magnetic* field, which has a node at an AC electric field maximum of the resonator.

Decay of the AC electric field beyond a thin surface layer of the sample (the skin effect) presents another challenge for the electric excitation of spin resonance. This issue may be bypassed by working with films [27] thinner than the skin depth. In the relevant frequency range of 10 GHz, the skin depth of a good metal such as chromium is of the order of one μm. Lowering the carrier concentration increases the skin depth: for various organic conductors and underdoped cuprates in the 10 GHz range, the skin depth measures dozens of μm [28, 29].

Previous studies of EDSR in semiconductors (see Refs. [15, 30, 31]) focused on relativistic spin-orbit interaction terms, those that appear in the absence of magnetic field. By contrast, in an antiferromagnet, the Zeeman spin-orbit coupling $\mathcal{H}_{ZSO}$ of Eqn. (1) is proportional to the magnetic field, which renders ZEDR tunable. Yet, as shown above, ZEDR becomes strong already in a weak field, which turns it into a promising experimental tool.

ZEDR offers a new method to investigate the coupling between electron spin and its orbital motion in antiferromagnets. Materials from chromium to borocarbides, cuprates, iron pnictides, organic and heavy fermion compounds may be studied using this phenomenon, and per-

haps employed to manipulate and monitor carrier spin with electric field.

I thank I. Aleiner, B. Altshuler, S. Brazovskii and L. P. Pitaevskii for enlightening discussions, and S. Carr, Ya. Bazaliy, N. Shannon, A. Shengelaya, T. Vekua, J. Wykhoff and S. Zvyagin for helpful comments. Parts of this work were done at the Max-Planck Institute for the Physics of Complex Systems in Dresden, at LPTMS in Orsay, and at the Institut Henri Poincare-Centre Emile Borel in Paris. I thank LPTMS, MPI PKS and IHP for the kind hospitality, and IFRAF for its generous support.

[1] *Semiconductor Spintronics and Quantum Computation*, edited by D. D. Awschalom, D. Loss, N. Samarth (Springer, Berlin 2002).
[2] *Concepts in Spin Electronics*, edited by S. Maekawa (Oxford University Press, New York 2006).
[3] I. Žutić, J. Fabian, S. Das Sarma, Rev. Mod. Phys. **76**, 323 (2004).
[4] S. Methfessel and D. C. Mattis, in *Magnetic Semiconductors*, Handbuch der Physik Vol. 18, edited by S. Flügge (Springer-Verlag, Berlin, 1968), p. 1.
[5] T. Jungwirth, J. Sinova, J. Mašek, J. Kučera, A. H. MacDonald, Rev. Mod. Phys. **78**, 809 (2006).
[6] *Spin Dependent Transport in Magnetic Nanostructures*, edited by S. Maekawa and T. Shinjo (Advances in Condensed Matter Science, Taylor & Francis, 2002).
[7] E. I. Rashba, Physica E **20**, 189 (2004).
[8] S. A. Brazovskii and I. A. Luk'yanchuk, Zh. Eksp. Teor. Fiz. **96**, 2088 (1989) [Sov. Phys. JETP **69**, 1180 (1989)].
[9] R. Ramazashvili, Phys. Rev. Lett. **101**, 137202 (2008).
[10] R. Ramazashvili, Phys. Rev. B **79**, 184432 (2009).
[11] A. N. Lavrov, H. J. Kang, Y. Kurita, T. Suzuki, Seiki Komiya, J. W. Lynn, S.-H. Lee, Pengcheng Dai, and Yoichi Ando, Phys. Rev. Lett. **92**, 227003 (2004).
[12] M. Matsuda, Y. Endoh, K. Yamada, H. Kojima, I. Tanaka, R. J. Birgeneau, M. A. Kastner and G. Shirane, Phys. Rev. B **45**, 12548 (1992).
[13] At first sight, the longitudinal and the transverse term in Eqn. (2) transform differently under inversion $\mathcal{I}$. However, ξ also has odd parity (see Refs. [9, 10]), thus removing the issue.
[14] I. S. Gradshtein, I. M. Ryzhik, *Table of Integrals, Series, and Products* (Academic Press, 2000).
[15] E. I. Rashba, V. I. Sheka, in *Landau Level Spectroscopy*, edited by G. Landwehr and E. I. Rashba (Elsevier Science Publishers B.V., 1991).
[16] In a weak field, transitions to other Landau levels are suppressed by even powers of $\left[\frac{\xi}{l_H}\right]^2 \ll 1$.
[17] ZEDR has been predicted in Ref. [19]. However, the result for absorption in a quantizing field, given in this article, overlooks the fact, that both the Landau level splitting and the absorption vanish in a purely transverse field.
[18] For comparison, cyclotron resonance matrix elements in a magnetic field of one Tesla are defined by $l_H \approx 26$ nm.
[19] R. Ramazashvili, Zh. Eksp. Teor. Fiz. **100**, 915 (1991) [Sov. Phys. JETP **73**, 505 (1991)].
[20] A. Shengelaya, H. Keller, K. A. Müller, B. I. Kochelaev, K. Conder, Phys. Rev. B **63**, 144513 (2001).
[21] At the same field $\Omega_0 \sim \frac{\Delta^2}{\epsilon_F}$, the relevant values of $\frac{\xi p_y}{\hbar}$ become of the order of unity, and the expansion of $g_\perp(\mathbf{p})$ breaks down together with the analytic results above.
[22] E. Fawcett, Rev. Mod. Phys. **60**, 209 (1988).
[23] Ravi K. Kummamuru & Yeong-Ah Soh, Nature **452**, 859 (2008), and references therein.
[24] F. Ronning *et al.*, Phys. Rev. B **67**, 165101 (2003).
[25] N. P. Armitage *et al.*, Phys. Rev. Lett. **88**, 257001 (2002).
[26] F. Keffer and C. Kittel, Phys. Rev. **85**, 329 (1952).
[27] H. Zabel, J. Phys.: Condens. Matter **11**, 9303 (1999).
[28] Yugo Oshima, PhD thesis, Kobe University (2003).
[29] M. R. Trunin, Usp. Fiz. Nauk **175**, 1017 (2005) [Physics-Uspekhi **48**, 979 (2005)].
[30] A. Shekhter, M. Khodas, A. M. Finkelstein, Phys. Rev. B **71**, 165329 (2005).
[31] M. Duckheim and D. Loss, Nature Physics **2**, 195 (2006).